Topological Equilibria of Ion Channel Peptides in Oriented Lipid Bilayers Revealed by ^{15}N Solid-State NMR Spectroscopy†

U. S. Sudheendra and Burkhard Bechinger*

Faculté de Chimie, Institut le Bel, Université Louis Pasteur/CNRS FRE2446, 4, rue Blaise Pascal, 67070 Strasbourg, France, and Max-Planck-Institut für Biochemie, Am Klopferspitz 18A, 82152 Martinsried, Germany

Received May 11, 2005; Revised Manuscript Received July 19, 2005

ABSTRACT: Ion channel peptides have been prepared by solid-phase peptide synthesis, labeled with ^{15}N at selected sites, and reconstituted into oriented lipid bilayers. The (Leu-Ser-Ser-Leu-Leu-Ser-Leu)$_3$-CONH$_2$ peptide has previously been shown to exhibit well-defined and discrete ionic conductances when investigated by single-channel measurements [Lear, J. D., et al. (1988) *Science 240*, 1177]. Proton-decoupled ^{15}N solid-state NMR spectroscopy indicates that (Leu-Ser-Ser-Leu-Leu-Ser-Leu)$_3$-CONH$_2$ preferentially aligns parallel to the membrane surface in excellent agreement with its amphipathic helical structure. However, by carefully choosing the conditions of the membrane environment, significant contributions that are indicative of transmembrane alignments become obvious in the ^{15}N chemical shift solid-state NMR spectra. The data thereby provide experimental evidence for an equilibrium between in-plane and transmembrane-oriented helix configurations where the transmembrane and surface-oriented peptide fractions are in slow exchange. Similar topological equilibria are observed when the N-terminus of the LS21 peptide is acetylated. These observations provide experimental support for previous models, suggesting that the channels observed in single-channel conductance measurements are indeed formed by hexameric transmembrane helical bundles. In contrast, the shorter peptide (Leu-Ser-Ser-Leu-Leu-Ser-Leu)$_2$-CONH$_2$ is oriented parallel to the membrane surface under all conditions tested. This peptide exhibits erratic conductance changes when investigated by electrophysiological methods, probably because it is too short to span the lipid bilayer.

Membrane channel proteins fulfill important functions during cellular signal transduction, neuronal excitability, muscle function, and many other important physiological processes. Defects associated with these proteins can have severe pathological consequences, a prime example being the putative chloride channel involved in cystic fibrosis. Unfortunately, membrane proteins are difficult to purify in quantitative amounts, and the common structural techniques often fail. Therefore, very little high-resolution structural information is available for channel proteins (*1*−*7*).

To elucidate some of the requirements of pore formation in structural detail, peptides that are known to increase the conductivity across phospholipid bilayers, such as alamethicin or melittin (*8*−*12*), have been extensively studied in the past. Furthermore, protein domains that are thought to line the pore of large channel proteins have been prepared and studied by structural methods (reviewed in refs *13*−*20*). Although small, these peptides exhibit a dynamic and complex behavior within the "soft" membrane environment. To further simplify matters, synthetic organic model compounds or minimalist peptide sequences have been designed, prepared, and studied by biophysical methods (*21*−*26*).

Among those, the (LSSLLSL)$_3$ peptide first presented by de Grado and co-workers has been investigated in considerable detail (*23*). This peptide has been designed with the potential to form an amphipathic α-helix in membrane environments. Assembling these helices without including charged amino acid side chains increased the possibility that they assemble into ion-conducting transmembrane helical bundles. In this configuration the serines line a water-filled channel and help in the solvation of passing ions (*27*). At the same time the leucines remain in contact with the hydrophobic membrane interior.

In planar lipid bilayer experiments the presence of transmembrane potentials causes the (LSSLLSL)$_3$ peptide to form discrete openings which exhibit conductivities of predominantly 70 pS [0.5 M KCl, −100 mV (*28*)]. More channels are formed at *cis*-negative voltages, a finding that is suggestive that the peptide inserts into the membrane with its C-terminus first (*28*). These studies also reveal a 10-fold increase in lifetime when the N-terminal amino group of the peptide is acetylated, as this reduces the electrostatic repulsion by like charges within the ion-conducting complex (*28*). The electrophysiological properties together with molecular modeling calculations suggest that the predominant channel structure is a transmembrane helical bundle of six parallel α-helices enclosing a channel diameter of about 8 Å (*23*, *28*). The channels are moderately cation-selective, an observation attributed to the alignment of serine side chains along the pore lumen (*28*). The rectifying properties of this and related channels correlate with the configuration of the α-helix macrodipole (*29*). Furthermore, the ion conductivities through such a hexameric channel have been modeled using computational methods (*30*, *31*).

† We acknowledge the Max-Planck-Society and the Région Alsace for funding the studentships attributed to U.S.S.

* Address correspondence to this author at the Faculté de Chimie, Institut le Bel. Tel: +33 3 90 24 51 50. Fax: +33 3 90 24 51 51. E-mail: bechinger@chimie.u-strasbg.fr.

10.1021/bi050866n CCC: $30.25
Published on Web 08/19/2005

However, when tryptophan derivatives of the peptides were investigated by fluorescence spectroscopy, the peptide has been found to insert into the membrane with a predominant orientation parallel to the membrane surface (*27*). In contrast, no direct structural evidence has, to our knowledge, so far been published for the postulated transmembrane orientations of these peptides. Notably, increases in membrane conductance have previously been observed also for charged peptides that are very unlikely to adopt stable transmembrane alignments at the peptide concentrations used during channel measurements (reviewed in refs *32* and *33*). It is, therefore, desirable to have further experimental evidence for the proposed model.

Proton-decoupled ^{15}N solid-state NMR[1] spectroscopy has a proven record during the investigation of interactions of polypeptide α-helices with oriented or nonoriented phospholipid bilayers (recently reviewed in ref *33*). Whereas ^{15}N chemical shifts <100 ppm are indicative of helix alignments approximately parallel to the membrane surface, values >180 ppm are associated with transmembrane orientations (*34*). By introducing a nonperturbing ^{15}N label into the peptide backbone, the method can thus be used to investigate the membrane alignments of these sequences. When the ^{15}N chemical shift measurement is combined with solid-state NMR measurables obtained from other nuclei, a very detailed analysis of the structure and topology of membrane associated peptides can be obtained (e.g., refs *35* and *36*). The oriented solid-state NMR technique works with extended lipid membranes and has been applied to study membrane-inserted peptide channels and antibiotics (*33*, *35*, *37*−*39*), lytic peptides (*40*), and model sequences (*33*), as well as membrane-associated proteins (*41*).

When we used this technique to investigate LS sequences in DOTAP bilayers, a lipid also used for transporting DNA and polypeptides into cells (*42*), a tendency of the LS21 peptide to adopt TM alignments has been observed. We therefore decided to investigate the lipid−peptide interactions of these peptides in a more systematic manner. In this paper LS14, LS21, and AcLS21 have been prepared and reconstituted in DOTAP, DPhPC, or DOPC membranes, and their alignment has been studied under a variety or different conditions. The implications of our results for the proposed model of channel formation will be discussed.

MATERIALS AND METHODS

Phospholipids were purchased from Avanti Polar Lipids (Alabaster, AL). Peptides LS14 [$(LSLLSSL)_2$], LS21 [$(LSLLSSL)_3$], and Ac-LS21 [*N*-acetyl-$(LSLLSSL)_3$] were prepared by solid-phase peptide synthesis on a Millipore 9050 automatic peptide synthesizer using Fmoc (9-flourenylmethyloxycarbonyl) chemistry (*43*, *44*) and a TentaGel SRAM-Leu-Fmoc resin (RAPP Polymer, Tübingen, Germany) with which C-terminal amides are obtained after the cleavage reaction. Despite the apparent simplicity in composition of the heptad repeat (Figure 1) the chemical preparation of quantitative amounts of the LS21 sequence has proven difficult to achieve in the past (e.g., ref *27*). Therefore, the standard synthetic protocols of this peptide synthesizer were modified by including double couplings for serines 3, 6, 10, and 13 and, more importantly, by applying the novel "pseudoproline" technology (*45*) at the serine−serine positions [Fmoc-Ser(tBu)-Ser(ψ-MePro)-OH from Novabiochem, VWR International, Fontenay sous Bois, France]. In this manner the yield of the LS21 synthesis could be much improved when compared to the individual addition of serines. At position 7 of LS14 and at position 12 of LS21, respectively, the ^{15}N-labeled derivative of leucine was inserted (Cambridge Isotopes Inc., Andover, MA). About 200 mg of crude synthetic products was obtained, which were purified by reversed-phase high-performance liquid chromatography using an acetonitrile/water gradient and a Prontosil 300-5-C4 5.0 μm column (Bischoff Chromatography, Leonberg, Germany). The yields after purification were 55% and 72% for LS21 and LS14, respectively. The identity and purity of the synthesized peptides were analyzed by using the matrix-assisted laser desorption ionization mass spectrometry (MALDI-MS) and analytical reversed-phase HPLC. The cationic lipid 1,2-dioleoyl-3-(trimethylammonium)propane (DOTAP) as well as the zwitterionic phospholipids 1,2-dioleoyl-*sn*-glycero-3-phosphocholine (DOPC) and 1,2-diphytanoyl-*sn*-glycero-3-phosphocholine (DPhPC) were purchased from Avanti Polar Lipids (Alabaster, AL).

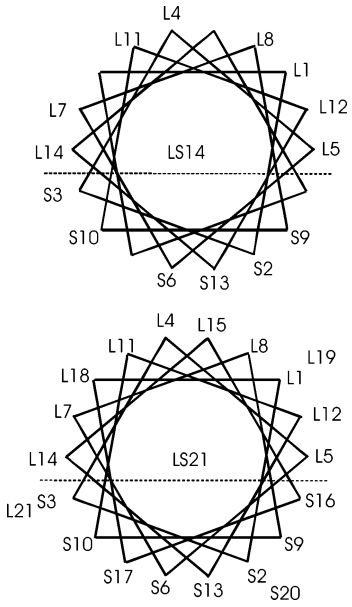

FIGURE 1: Edmundson helical wheel diagram of LS14 and LS21.

To reconstitute the peptides into oriented lipid bilayers, typically 7−16 mg of peptide was dissolved in trifluroethanol/water (4 mL/0.3 mL) and mixed with 200 mg of lipid in dichloromethane. Unless indicated otherwise, the peptide-to-lipid molar ratios were 2 mol %. The solutions thus obtained were clear and homogeneous. During the preparation the pH of the sample was set to the indicated pH values using Tris buffer and 1 N NaOH. The lipid−peptide mixture was applied onto 30 ultrathin cover glasses (9×22 mm; Paul Marienfeld GmbH & Co. KG, Lauda-Königshofen, Germany), first dried in air and thereafter in high vacuum overnight (1.8×10^{-2} mbar). The samples were equilibrated

[1] Abbreviations: DPhPC, 1,2-diphytanoyl-*sn*-glycero-3-phosphocholine; DOPC, 1,2-dioleoyl-*sn*-glycero-3-phosphocholine; DOTAP, 1,2-dioleoyl-3-(trimethylammonium)propane; fwhm, full width at half-maximum; IP, in-plane; LS14, $(Leu\text{-}Ser\text{-}Ser\text{-}Leu\text{-}Leu\text{-}Ser\text{-}Leu)_2$-$CONH_2$; LS21, $(Leu\text{-}Ser\text{-}Ser\text{-}Leu\text{-}Leu\text{-}Ser\text{-}Leu)_3$-$CONH_2$; Ac-LS21, *N*-acetyl-$(Leu\text{-}Ser\text{-}Ser\text{-}Leu\text{-}Leu\text{-}Ser\text{-}Leu)_3$-$CONH_2$; NMR, nuclear magnetic resonance; TM, transmembrane.

in a closed chamber where a defined relative humidity is obtained due to contact with saturated salt solutions of KNO_3 (93% relative humidity), NH_4NO_3 (84% relative humidity), or NH_4Cl (75% relative humidity), respectively (*46*). After 3−5 days the glass plates were stacked on top of each other. The stacks were stabilized and sealed with Teflon tape and plastic wrappings.

For solid-state NMR spectroscopy the samples were introduced into the flattened coils (*47*) of a double-resonance probe and inserted into the magnetic field (9.4 T) of a Bruker Avance 400 wide-bore solid-state NMR spectrometer. The sample was oriented with the membrane normal parallel to the B_0 field of the spectrometer. Proton-decoupled ^{15}N solid-state NMR spectra were acquired using the MOIST cross-polarization pulse sequence (*48*). The static solid-state NMR spectra were acquired using the following parameters: ^1H B_1 field of approximately 1 mT, 1 ms contact time, 3 s recycle delay, 37 kHz spectral width, 512 data points, and number of acquisitions typically 25000−35000. During acquisition the sample was cooled with a stream of air at room temperature. An exponential apodization function corresponding to a line broadening of 200 Hz was applied before Fourier transformation. NH_4Cl (41.5 ppm) was used as a reference corresponding to approximately 0 ppm for liquid NH_3.

The tilt and rotational pitch angles that agree with the measured ^{15}N chemical shift were calculated according to ref *36*.

RESULTS

The LS14 and the LS21 channel peptides were prepared by solid-phase peptide synthesis, labeled with ^{15}N at a single backbone site within the central part of the polypeptide, reconstituted into uniaxially oriented lipid bilayers, and investigated by proton-decoupled ^{15}N solid-state NMR spectroscopy. Using CD and tryptophan fluorescence spectroscopies it has been shown previously that these and other amphipathic peptides adopt α-helical conformations in membrane environments (*23*, *27*, *32*).

Figure 2B shows the proton-decoupled ^{15}N solid-state NMR spectra of 2 mol % LS21 when reconstituted in DOPC lipid bilayers. The spectrum of the ^{15}N-labeled leucine at position 12 of the LS21 peptide is characterized by a single peak at 63 ppm. This value is indicative of an orientation of the helix long axis parallel to the membrane surface (*34*). Notably, the resonance is characterized by a broad line shape that extends into the 100 ppm region.

For comparison, the proton-decoupled ^{15}N solid-state NMR spectrum of a powder of dry LS21 is shown in Figure 2A. In this sample all orientations are present at random, and the spectrum therefore represents the full ^{15}N chemical shift anisotropy of the labeled amide bond covering approximately 175 ppm (*49*−*53*). The "hole" observed in the central region of the spectrum is probably due to the orientation dependence of $^1H-^{15}N$ dipolar interactions which are smallest close to the magic angle, concomitant with decreased cross-polarization efficiency at these frequencies.

To test for the effects on the topology of LS21 of the composition of the lipid fatty acyl chains, the LS21 peptide was also reconstituted into DPhPC lipid bilayers. This lipid forms electrically well-insulated membranes and was, therefore, used during the electrophysiological investigations of LS21 and LS14 (*23*). The ^{15}N chemical shift line shape of this sample is, within experimental error, identical to the one obtained in the presence of DOPC membranes (Figure 2C). When the pH is decreased to 7.5, the ^{15}N chemical shift value of 64 ± 3 ppm remains unaffected (not shown).

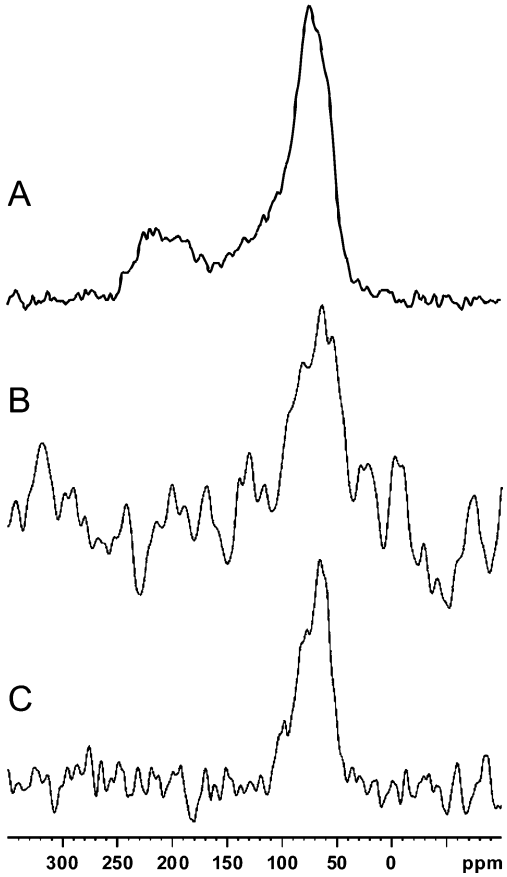

FIGURE 2: Proton-decoupled ^{15}N NMR solid-state NMR spectra of LS21: (A) dry powder, (B) 2 mol % LS21 reconstituted in DOPC at pH 8.5 and 93% relative humidity, and (C) same as (B) except reconstituted in DPhPC.

Furthermore, the effects on the topology of LS21 of the composition of the lipid headgroup region was tested by reconstitution into DOTAP lipid bilayers. Figure 3A shows the proton-decoupled ^{15}N solid-state NMR spectra of 2 mol % LS21 when inserted in DOTAP lipid bilayers at pH 7.5. The spectrum of the ^{15}N-labeled leucine at position 12 of the LS21 peptide is characterized by a single peak at 65 ppm. This value is indicative of an orientation of the helix long axis parallel to the membrane surface (*34*). The resonance is characterized by a narrow line shape with full width at half-maximum (fwhm) of 8 ppm, indicative of a well-defined tilt angle of this peptide. Figure 4 indicates the combinations of tilt and rotational pitch angles that are in agreement with a ^{15}N chemical shift value of 65 (inner contour) or 70 ppm (outer contour), indicating the orientational restraints that are obtained with this measurement. When the peptide-to-lipid ratio is increased to 1/20, the ^{15}N broadens, indicating a more heterogeneous alignment of the peptide relative to the magnetic field direction (Figure 3B).

The increased dispersion in ^{15}N chemical shift values observed when LS21 is reconstituted into phosphatidylcholine or at high peptide-to-lipid ratios into DOTAP membranes is indicative of macroscopic distortions of the membrane,

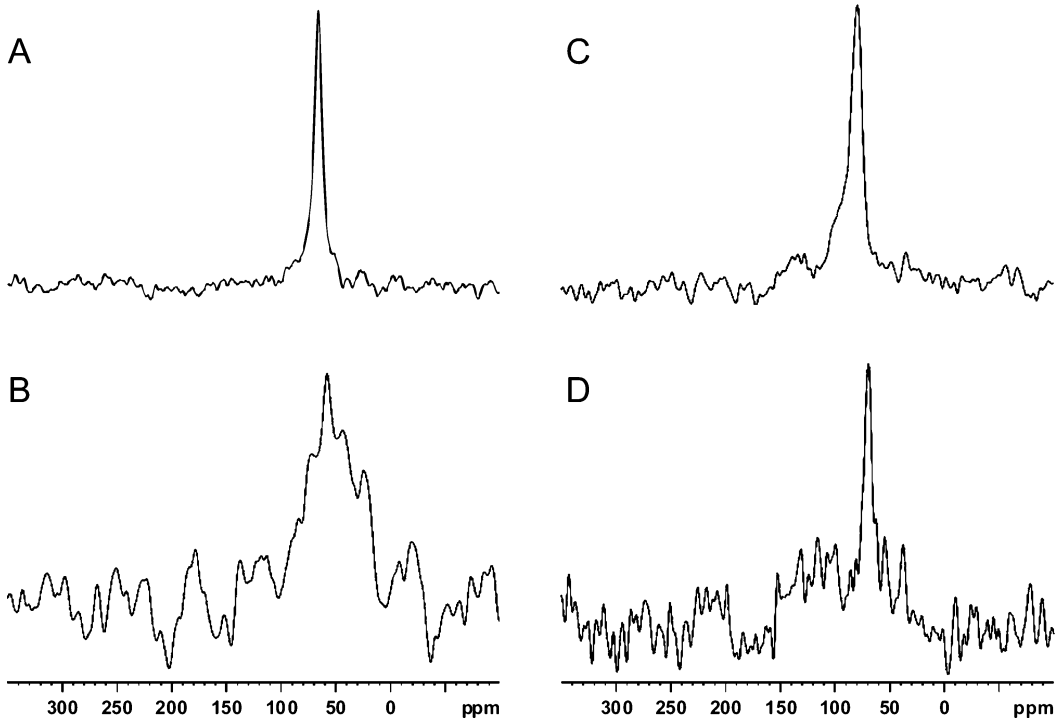

FIGURE 3: Proton-decoupled ^{15}N NMR solid-state NMR spectra of LS21 in DOTAP lipid membranes equilibrated at 93% relative humidity: (A) pH 7.5, 2 mol %, (B) pH 7.5, 5 mol %, (C) pH 6.5, 2 mol %, and (D) 2 mol % of the N-acetylated peptide at pH 6.5. Only 7000 and 13000 scans were acquired for spectra B and D, respectively.

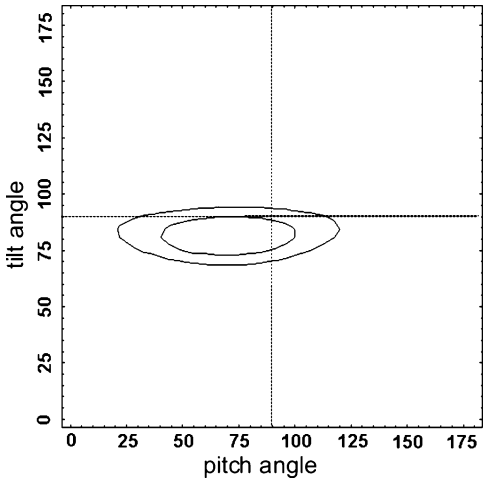

FIGURE 4: Analysis of the helix orientations of [^{15}N-Leu12]-LS21 that agree with a ^{15}N chemical shift value of 65 ± 5 ppm. The inner contour corresponds to the measured value (Figure 3A) and the outer contour to 70 ppm.

peptide conformational changes, modifications in the distribution of alignments, exchange between isotropic and oriented peptide configurations, and/or alterations in the exchange rates between peptide structures and topologies. Indeed, proton-decoupled ^{31}P NMR spectra of the DOPC samples exhibit additional signal intensities reaching to −17 ppm, which is indicative of pronounced distortions in DOPC phospholipids headgroup orientations due to the presence of LS21 (not shown). In analogy with other amphipathic peptide preparations from our laboratory we suggest that the bilayer alignment is disturbed due to the high density of interfacial insertion of LS21 peptides (*54*).

In a next step we investigated the effect of pH and degree of hydration on the topology of the LS21 peptide when reconstituted into oriented DOTAP lipid bilayers (Figure 5). At pH 8.5 and 93% relative humidity two signal intensities at 79 and 217 ppm are visible at a ratio of approximately 1:1 (Figure 5A). This result indicates the coexistence of in-plane and transmembrane peptide orientations. Notably, exchange between these configurations is slow on the time scale of the ^{15}N chemical shift anisotropy (10^{-4} s). When this sample is dehydrated, the equilibrium between in-plane and the transmembrane-oriented peptide shifts in favor of the former one (Figure 5). After the sample has been equilibrated at reduced hydration levels of 84% and 75% relative humidity, respectively, the ^{15}N NMR peak intensity at 79 ppm dominates, although significant intensities in the 217 ppm region remain (Figure 5B,C).

To test if interactions between the positive surface charge density of the DOTAP lipid bilayer and the cationic N-terminus of the peptide affect its interactions with the membrane, an LS21 sequence was prepared with the N-terminus acetylated. After reconstitution of Ac-LS21 at pH 8.5 and equilibration at 93% relative humidity a distribution of transmembrane and in-plane alignments was obtained (Figure 5D) comparable to the one observed for LS21 (Figure 5A−C).

Additional spectra were recorded of LS21 and Ac-LS21 after reconstitution into DOTAP lipid bilayers at pH 6.5 at a peptide-to-lipid ratio of 2 mol %. The ^{15}N spectra are characterized by narrow line shapes at 79 and 69 ppm with fwhm of about 10 ppm, respectively (Figure 3C,D). These data confirm the unique and well-defined alignment of LS21 observed also at pH 7.5 (Figure 3A).

Finally, the peptide encompassing only two leucine−serine heptad repeats (LS14) was investigated. An α-helical peptide of this length is generally believed to be too short to span a biological membrane (*23*). Indeed, when LS14 is reconstituted in DOTAP lipid bilayers at pH 7.5 and 93% relative humidity, the proton-decoupled ^{15}N solid-state NMR spec-

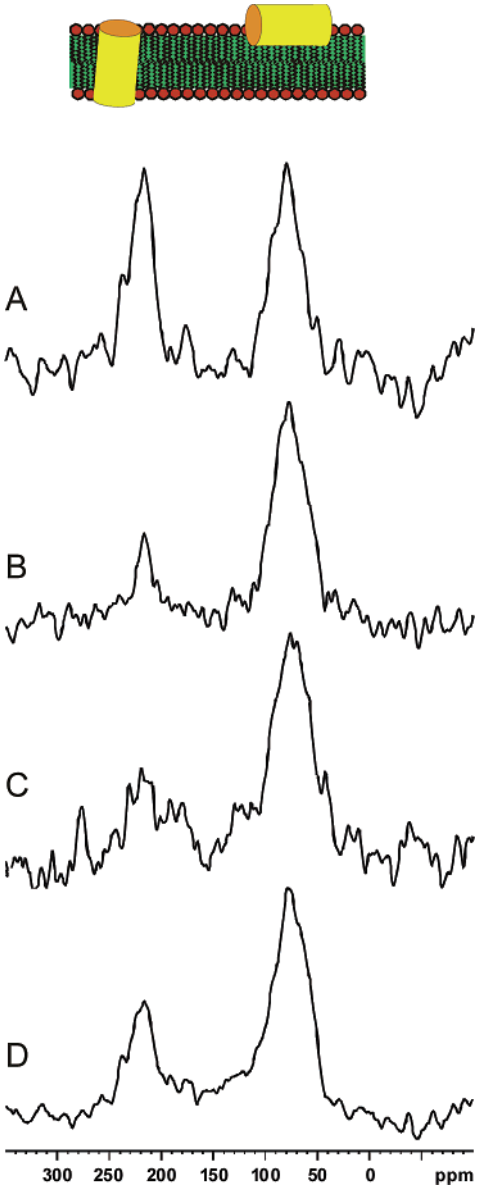

FIGURE 5: Proton-decoupled ^{15}N NMR solid-state NMR spectra of 2 mol % LS21 peptide reconstituted in DOTAP membranes at pH 8.5 at (A) 93% relative humidity, (B) 84% relative humidity, and (C) 75% relative humidity, and (D) Ac-LS21, same conditions as (A). The relationship between helix orientation and chemical shift scale is illustrated (on top).

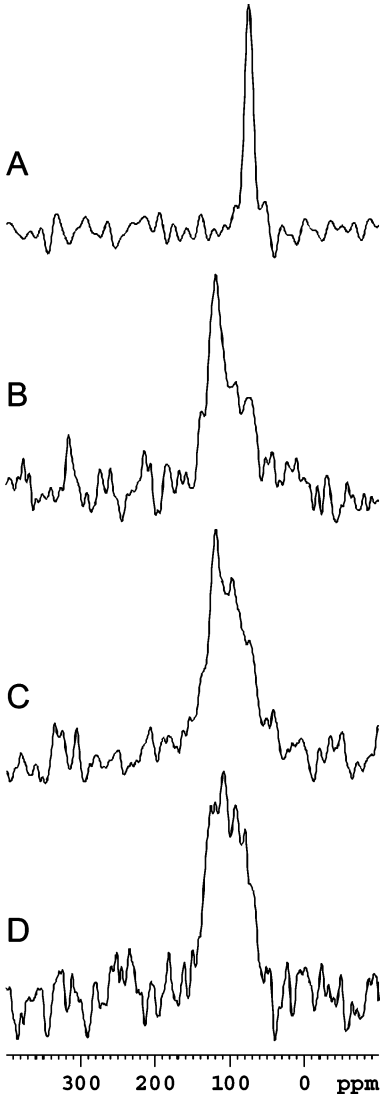

FIGURE 6: Proton-decoupled ^{15}N NMR solid-state NMR spectra of 2 mol % LS14 peptide reconstituted in DOTAP bilayer: (A) pH 7.5 and 93% relative humidity, (B) pH 8.5 and 93% relative humidity, (C) pH 8.5 and 84% relative humidity, and (D) pH 8.5 and 75% relative humidity.

trum is characterized by a narrow signal at 75 ppm with fwhm of 13 ppm/0.5 kHz (Figure 6A). This result is indicative of a well-defined alignment of this helix parallel to the membrane surface. When the pH of this sample is increased to 8.5, the main peak intensity is shifted to 119 ppm, which corresponds to the isotropic value of leucine amides (*49*, *50*, *55*, *56*); albeit significant signal intensities also remain in the 70 ppm region. When the degree of hydration is reduced, resonance intensities remain between 120 and 70 ppm, when at the same time the mean of the ^{15}N signal intensity shifts toward the low-field end of the NMR spectrum (Figure 6B,C).

DISCUSSION

The LS21 and LS14 peptides have been designed to form amphipathic helices in membrane environments (*23*). The LS21 peptide has been shown to exhibit channel properties in DPhPC membranes, thereby resembling the fungal peptide alamethicin or large channel proteins (*9*, *23*). This peptide has, therefore, been suggested to be a model for proteins forming transmembrane helical bundles, in particular when transmembrane electrical potentials are applied (*27*, *28*). The channel properties of its N-acetylated form exhibit 10 times longer channel lifetimes and have been investigated in even greater detail in electrophysiological experiments (*29*, *57*, *58*).

On the other hand, LS14 is too short for such an arrangement and, therefore, only induces stochastic currents when added to planar lipid bilayers (*23*). Other amphipathic peptides which carry many lysines at their hydrophilic face have initially been suggested to also form TM channels; however, a considerable amount of experimental data shows that neither the channel properties nor the structural and topological characteristics agree with such a model (reviewed in ref *32*). Furthermore, theoretical estimates of the energies involved in associating a large number of charged residues in a small channel volume indicate a high energetic penalty when such a TM helical bundle is formed (*11*). Other models

such as the carpet model or the detergent-like mode of action have therefore been suggested to be the underlying mechanism for these highly charged peptides (*32*, *59*). However, in the case of LS21 the hydrophilic side of the amphipathic helix is composed of polar but uncharged serines, and the formation of transmembrane helical bundles seems to present a reasonable model (*28*). In this paper we, therefore, tested the alignment of LS peptides in lipid bilayers of variable composition using proton-decoupled ^{15}N solid-state NMR on oriented membranes (*33*).

The ^{15}N chemical shift <100 ppm, which was observed for the LS peptides in all the samples tested (Figures 2−6), indicates that an alignment parallel to the membrane surface is the preferred configuration of this series of amphipathic peptides. The data are in excellent agreement with static fluorescence quenching experiments which suggest an in-plane alignment of LS21 and a location of the helix axis a few angstroms below the polar headgroup/hydrocarbon boundary (*27*). This in-plane arrangement ideally reflects the perfect amphipathic separation of polar and hydrophobic residues (Figure 1) as it allows the polar serine residues to be exposed to the water phase when at the same time the leucines are immersed in the bilayer interior. In a similar manner other amphipathic helices with charged side chains and/or with high hydrophobic moment have been found oriented parallel to the membrane surface (*60*−*62*). In contrast, sequences composed of leucine and alanines or of leucines alone adopt stable transmembrane alignments, even though, to our knowledge, channel formation has so far not been demonstrated for these hydrophobic model sequences (*63*−*67*).

When LS21 is reconstituted into cationic DOTAP lipid membranes at pH 8.5, an additional signal intensity >200 ppm is observed (Figure 5). This result indicates the coexistence of surface and transmembrane-oriented peptides, which are in slow exchange on the 10^{-4} s time scale. The observed variations in LS21−lipid interactions and in orientational mosaic spread in different lipid environments (Figures 2, 3, and 5) are probably related to the alterations in packing constraints at the level of the phospholipid headgroups. Whereas the small size of the DOTAP headgroup provides an explanation why transmembrane insertion is observed for this but not phosphatidylcholine lipids, the pH dependence is more difficult to explain. However, the dependence of the observed topologies on hydration (Figure 5A−C) suggests that subtle shifts in the environment, such as changes in the structure of the lipid-associated water, modified H-bonding interactions, differences in the ionic composition of the buffer, or combinations thereof are involved. Notably, changes in the ΔG of transition of only a few kilojoules per mole are sufficient to shift the IP to TM equilibria (cf. below).

In contrast, the LS14 peptide is too short to span the lipid membrane and remains surface-associated at this and other conditions tested (Figure 6). Considerable ^{15}N signal intensities reach into the "isotropic" region of the ^{15}N chemical shift dispersion, in particular when the degree of hydration is increased (Figure 6). These data suggest that LS14 is associated with the lipid interface but in conformational and/or topological exchange with the membrane-associated water layer.

The ensemble of data can thus be explained by a model where peptides in the water phase are in dynamic exchange with membrane-inserted configurations. In the membrane-associated state the LS21 sequences can adopt in-plane (IP) or transmembrane (TM) alignments (*68*, *69*). Oriented ^{15}N solid-state NMR experiments as well as a variety of other biophysical experiments have previously been used to demonstrate the existence of IP $\leftrightarrow$ TM equilibria of peptaibols (*70*, *71*) and melittin (*40*, *72*, *73*, *74*), as well as pH-dependent peptide antibiotics and model sequences (reviewed in ref *62*).

Furthermore, LS21 has been shown to exist as an equilibrium mixture of monomers and dimers in the absence of a voltage gradient across the bilayer (*27*). In a simplified manner these exchange processes can be represented by the equation (cf. also TOC graphics): aggregates in the aqueous phase $\leftrightarrow$ ... $\leftrightarrow$ membrane surface associated $\leftrightarrow$ IP $\leftrightarrow$ TM. Within these general definitions subequilibria such as

$$IP_1 \leftrightarrow IP_2 \leftrightarrow ...$$

or

$$TM_1 \leftrightarrow TM_2 \leftrightarrow ... \leftrightarrow TM_n$$

exist, where the indices indicate the number of associated monomers. A parallel bundle of six transmembrane helices (TM_6) has been modeled as the predominant channel observed in electrophysiological experiments (*28*). Within this framework the exchange between weakly surface associated (isotropic on the NMR time scale) and IP-oriented LS14 (Figure 6) as well as between IP and TM aligned LS21 (Figure 5) can be explained.

The close to 1:1 distribution of ^{15}N signals <100 ppm and >200 ppm visible in Figure 5A indicates that the IP $\leftrightarrow$ TM equilibrium is governed by a difference in Gibbs free energy close to zero under the conditions of the investigation. When we estimate that the signal-to-noise ratio of the ^{15}N solid-state NMR spectra allows us to detect a signal which encompasses at least 5% of the total intensity, the difference of the free energy describing this two-state equilibrium (ΔG) must not exceed ± 7.5 kJ/mol. This value indicates that relatively small energetic changes can indeed modify the distribution of signal intensities such as observed in Figures 2 and 4 when the membrane hydration level or the sample pH is changed. Notably, in our model the transmembrane topology is a requirement but not sufficient for pore formation, but needs to be followed by oligomerization of amphipathic helices. Whereas TM insertion of Ac-LS21 might be as good or even slightly less favorable when compared to LS21 (Figure 5), the electrostatic repulsion between these former helices is reduced and a more stable conductive pore is thus obtained (*31*).

In case of alamethicin channels it has been suggested that transmembrane electrical fields result in an increased partitioning of this peptide into the membrane (*75*), as well as a shift in the IP $\leftrightarrow$ TM equilibrium due to a reorientation of the helix macroscopic dipole (reviewed in refs *9* and *11*). A similar model has also been proposed for LS21 (*23*). Here we present direct experimental proof that transmembrane orientations of LS21 or other highly amphipathic peptides (*68*) occur in lipid bilayers as long as the number of charges carried by these peptides is limited. Therefore, the data

support the idea that transmembrane electric fields help to reorient a fraction of LS21 peptides (*27*), concomitant with the formation of transmembrane helical bundles and channel formation. The gating charge associated with this process has been measured to encompass 3.6 elementary charges in the case of LS21 (*28*). This corresponds to moving 0.6 elementary charge per monomer when a hexameric channel structure is considered. In a transmembrane electric field of 100 mV such a process is associated with a favorable energy contribution of about 5 kJ/mol (per monomer), i.e., according to the data presented in this paper (Figure 5), sufficient to significantly increase the number of transmembrane helical peptides. As a consequence, our results support the previously proposed model for the voltage-induced increases in ion conductivity (*23*).

ACKNOWLEDGMENT

We are most grateful to Josefine März, Gérard Nullans, and Monica Zabowa for help with peptide synthesis and mass spectrometric analysis. Furthermore, we acknowledge Ulrike Harzer for discussing the potential improvements in peptide synthesis by using pseudoprolines and Christopher Aisenbrey for help in preparing Figure 4, as well as Philippe Bertani and Jesus Raya for support at the NMR spectrometer.

REFERENCES

1. Doyle, D. A., Cabral, J. M., Pfuetzner, R. A., Kuo, A. L., Gulbis, J. M., Cohen, S. L., Chait, B. T., and MacKinnon, R. (1998) The structure of the potassium channel—Molecular basis of K^+ conduction and selectivity, *Science 280*, 69−77.
2. Oakley, A. J., Martinac, B., and Wilce, M. C. (1999) Structure and function of the bacterial mechanosensitive channel of large conductance, *Protein Sci. 8*, 1915−1921.
3. Leite, J. F., and Cascio, M. (2001) Structure of ligand-gated ion channels: critical assessment of biochemical data supports novel topology, *Mol. Cell. Neurosci. 17*, 777−792.
4. Rees, D. C., Chang, G., and Spencer, R. H. (2000) Crystallographic analyses of ion channels: lessons and challenges, *J. Biol. Chem. 275*, 713−716.
5. Bass, R. B., Locher, K. P., Borths, E., Poon, Y., Strop, P., Lee, A., and Rees, D. C. (2003) The structures of BtuCD and MscS and their implications for transporter and channel function, *FEBS Lett. 555*, 111−115.
6. Dutzler, R. (2004) The structural basis of ClC chloride channel function, *Trends Neurosci. 27*, 315−320.
7. Sorensen, T. L., Moller, J. V., and Nissen, P. (2004) Phosphoryl transfer and calcium ion occlusion in the calcium pump, *Science 304*, 1672−1675.
8. Dempsey, C. E. (1990) The actions of melittin on membranes, *Biochim. Biophys. Acta 1031*, 143−161.
9. Sansom, M. S. P. (1991) The biophysics of peptide models of ion channels, *Prog. Biophys. Mol. Biol. 55*, 139−235.
10. Woolley, G. A., and Wallace, B. A. (1992) Model ion channels: gramicidin and alamethicin, *J. Membr. Biol. 129*, 109−136.
11. Bechinger, B. (1997) Structure and functions of channel-forming polypeptides: magainins, cecropins, melittin and alamethicin, *J. Membr. Biol. 156*, 197−211.
12. Duclohier, H., and Pichon, Y. (2004) Ion channels: from biophysics to disorders, *Eur. Biophys. J. 33*, 167−168.
13. Spach, G., Duclohier, H., Molle, G., and Valleton, J. M. (1989) Structure and supramolecular architecture of membrane channel-forming peptides, *Biochimie 71*, 11−21.
14. Montal, M. (1995) Molecular mimicry in channel-protein structure, *Curr. Opin. Struct. Biol. 5*, 501−506.
15. Shai, Y. (1995) Molecular recognition between membrane-spanning polypeptides, *Trends Biochem. Sci. 20*, 460−464.
16. Haris, P. I. (1998) Synthetic peptide fragments as probes for structure determination of potassium ion-channel proteins, *Biosci. Rep. 18*, 299−312.
17. Bechinger, B. (2000) Understanding peptide interactions with lipid bilayers: a guide to membrane protein engeneering, *Curr. Opin. Chem. Biol. 4*, 639−644.
18. Arkin, I. T. (2002) Structural aspects of oligomerization taking place between the transmembrane alpha-helices of bitopic membrane proteins, *Biochim. Biophys. Acta 1565*, 347−363.
19. Tian, C., Gao, P. F., Pinto, L. H., Lamb, R. A., and Cross, T. A. (2003) Initial structural and dynamic characterization of the M2 protein transmembrane and amphipathic helices in lipid bilayers, *Protein Sci. 12*, 2597−2605.
20. DeGrado, W. F., Gratkowski, H., and Lear, J. D. (2003) How do helix-helix interactions help determine the folds of membrane proteins? Perspectives from the study of homo-oligomeric helical bundles, *Protein Sci. 12*, 647−665.
21. Heitz, F., and Spach, G. (1982) Ionic channels of some glycine-rich synthetic polypeptides, *Biochem. Biophys. Res. Commun. 105*, 179−185.
22. de Santis, P., Palleschi, A., Savino, M., Scipioni, A., Sesta, B., and Verdini, A. (1985) Poly(DL-proline), a synthetic polypeptide behaving as an ion channel across bilayer membranes, *Biophys. Chem. 21*, 211−215.
23. Lear, J. D., Wasserman, Z. R., and DeGrado, W. F. (1988) Synthetic amphiphilic peptide models for protein ion channels, *Science 240*, 1177−1181.
24. Iwata, T., Lee, S., Oishi, O., Aoyagi, H., Ohno, M., Anzai, K., Kirino, Y., and Sugihara, G. (1994) Design and synthesis of amphipathic 3_{10}-helical peptides and their interactions with phospholipid bilayers and ion channel formation, *J. Mol. Biol. 269*, 4928−4933.
25. Biron, E., Otis, F., Meillon, J. C., Robitaille, M., Lamothe, J., Van Hove, P., Cormier, M. E., and Voyer, N. (2004) Design, synthesis, and characterization of peptide nanostructures having ion channel activity, *Bioorg. Med. Chem. 12*, 1279−1290.
26. Gokel, G. W., Schlesinger, P. H., Djedovic, N. K., Ferdani, R., Harder, E. C., Hu, J., Leevy, W. M., Pajewska, J., Pajewski, R., and Weber, M. E. (2004) Functional, synthetic organic chemical models of cellular ion channels, *Bioorg. Med. Chem. 12*, 1291−1304.
27. Chung, L. A., Lear, J. D., and DeGrado, W. F. (1992) Fluorescence studies of the secondary structure and orientation of a model ion channel peptide in phospholipid vesicles, *Biochemistry 31*, 6608−6616.
28. Akerfeldt, K. S., Lear, J. D., Wassermann, Z. R., Chung, L. A., and DeGrado, W. F. (1993) Synthetic peptides as models for ion channel proteins, *Acc. Chem. Res. 26*, 191−197.
29. Lear, J. D., Schneider, J. P., Kienker, P. K., and DeGrado, W. F. (1997) Electrostatic effects on ion selectivity and rectification in designed ion channel peptides, *J. Am. Chem. Soc. 119*, 3212−3217.
30. Chen, D., Lear, J., and Eisenberg, B. (1997) Permeation through an open channel: Poisson−Nernst−Planck theory of a synthetic ionic channel, *Biophys. J. 72*, 97−116.
31. Dieckmann, G. R., Lear, J. D., Zhong, Q., Klein, M. L., DeGrado, W. F., and Sharp, K. A. (1999) Exploration of the structural features defining the conduction properties of a synthetic ion channel, *Biophys. J. 76*, 618−630.
32. Bechinger, B. (1999) The structure, dynamics and orientation of antimicrobial peptides in membranes by solid-state NMR spectroscopy, *Biochim. Biophys. Acta 1462*, 157−183.
33. Bechinger, B., Aisenbrey, C., and Bertani, P. (2004) Tolology, structure and dynamics of membrane-associated peptides by solid-state NMR spectroscopy, *Biochim. Biophys. Acta 1666*, 190−204.
34. Bechinger, B., and Sizun, C. (2003) Alignment and structural analysis of membrane polypeptides by ^{15}N and ^{31}P solid-state NMR spectroscopy, *Concepts Magn. Reson. 18A*, 130−145.
35. Cross, T. A. (1997) Solid-state nuclear magnetic resonance characterization of gramicidin channel structure, *Methods Enzymol. 289*, 672−696.
36. Aisenbrey, C., and Bechinger, B. (2004) Tilt and rotational pitch angles of membrane-inserted polypeptides from combined ^{15}N and ^{2}H solid-state NMR spectroscopy , *Biochemistry 43*, 10502−10512.
37. North, C. L., Barranger-Mathys, M., and Cafiso, D. S. (1995) Membrane orientation of the N-terminal segment of alamethicin determined by solid-state ^{15}N NMR, *Biophys. J. 69*, 2392−2397.
38. Bak, M., Bywater, R. P., Hohwy, M., Thomsen, J. K., Adelhorst, K., Jakobsen, H. J., Sorensen, O. W., and Nielsen, N. C. (2001) Conformation of alamethicin in oriented phospholipid bilayers

determined by N-15 solid-state nuclear magnetic resonance, *Biophys. J. 81*, 1684−1698.
39. Yamaguchi, S., Hong, T., Waring, A., Lehrer, R. I., and Hong, M. (2002) Solid-state NMR investigations of peptide-lipid interaction and orientation of a beta-sheet antimicrobial peptide, protegrin, *Biochemistry 41*, 9852−9862.
40. Smith, R., Separovic, F., Milne, T. J., Whittaker, A., Bennett, F. M., Cornell, B. A., and Makriyannis, A. (1994) Structure and orientation of the pore-forming peptide, melittin, in lipid bilayers, *J. Mol. Biol. 241*, 456−466.
41. Lambotte, S., Jasperse, P., and Bechinger, B. (1998) Orientational distribution of alpha-helices in the colicin B and E1 channel domains: A one- and two-dimensional ^{15}N solid-state NMR investigation in uniaxially aligned phospholipid bilayers, *Biochemistry 37*, 16−22.
42. Walker, C., Selby, M., Erickson, A., Cataldo, D., Valensi, J. P., and Van Nest, G. V. (1992) Cationic lipids direct a viral glycoprotein into the class I major histocompatibility complex antigen-presentation pathway, *Proc. Natl. Acad. Sci. U.S.A 89*, 7915−7918.
43. Atherton, E., Logan, C. J., and Sheppart, R. C. (1981) Peptide synthesis: Part 2. Procedures for solid-phase synthesis using N$^{\alpha}$-fluorenyllmethoxycarbonylamino acids on polyamide supports. Synthesis of substance P and of acyl carrier proteins 65−74 decapeptide, *J. Chem. Soc., Perkin Trans. 1*, 538−546.
44. Carpino, L. A., and Han, G. Y. (1972) The 9-fluorenylmethoxycarbonylamino-protecting group, *J. Org. Chem. 37*, 3404.
45. Haack, T., and Mutter, M. (1992) Serine derived oxazolidines as secondary structure disrupting, solubilizing building blocks in peptide synthesis, *Tetrahedron Lett. 33*, 1589−1592.
46. O'Brien, F. E. M. (1948) The control of humidity by saturated salt solutions, *J. Sci. Instrum. 25*, 73−76.
47. Bechinger, B., and Opella, S. J. (1991) Flat-coil probe for NMR spectrscopy of oriented membrane samples, *J. Magn. Reson. 95*, 585−588.
48. Levitt, M. H., Suter, D., and Ernst, R. R. (1986) Spin dynamics and thermodynamics in solid-state NMR cross polarization, *J. Chem. Phys. 84*, 4243−4255.
49. Oas, T. G., Hartzell, C. J., Dahlquist, F. W., and Drobny, G. P. (1987) The amide ^{15}N chemical shift tensors of four peptides determined from ^{13}C dipole-coupled chemical shift powder patterns, *J. Am. Chem. Soc. 109*, 5962−5966.
50. Hartzell, C. J., Whitfield, M., Oas, T. G., and Drobny, G. P. (1987) Determination of the ^{15}N and ^{13}C chemical shift tensors of L-[^{13}C]-alanyl-L-[^{15}N]alanine from the dipole-coupled powder patterns, *J. Am. Chem. Soc. 109*, 5966−5969.
51. Shoji, A., Ozaki, T., Fujito, T., Deguchi, K., Ando, S., and Ando, I. (1989) ^{15}N NMR chemical shift tensors and conformation of some ^{15}N-labeled polypeptides in the solid state, *Macromolecules 22*, 2860−2863.
52. Teng, Q., and Cross, T. A. (1989) The in situ determination of the ^{15}N chemical-shift tensor orientation in a polypeptide, *J. Magn. Reson. 85*, 439−447.
53. Lee, D. K., Wittebort, R. J., and Ramamoorthy, A. (1998) Characterization of ^{15}N chemical shift and ^{1}H-^{15}N dipolar coupling interactions in a peptide bond of uniaxially oriented and polycrystalline samples by one-dimensional dipolar chemical shift solid-state NMR spectroscopy, *J. Am. Chem. Soc. 120*, 8868−8874.
54. Bechinger, B. (2005) Detergent-like properties of magainin antibiotic peptides: A ^{31}P solid-state NMR study, *Biochim. Biophys. Acta* (in press).
55. Shoji, A., Ozaki, T., Fujito, T., Deguchi, K., Ando, S., and Ando, I. (1990) ^{15}N chemical shift tensors and conformation of solid polypeptides containing ^{15}N-labeled L-alanine residue by ^{15}N NMR. 2. Secondary structure reflected in s_{22}, *J. Am. Chem. Soc. 112*, 4693−4697.
56. Le, H., and Oldfield, E. (1994) Correlation between ^{15}N NMR chemical shifts in proteins and secondary structure, *J. Biomol. NMR 4*, 341−348.
57. Kienker, P. K., DeGrado, W. F., and Lear, J. D. (1994) A helical-dipole model describes the single-channel current rectification of an uncharged peptide ion channel, *Proc. Natl. Acad. Sci. U.S.A. 91*, 4859−4863.
58. Kienker, P. K., and Lear, J. D. (1995) Charge selectivity of the designed uncharged peptide ion channel Ac-(LSSLLSL)3-CONH$_2$, *Biophys. J. 68*, 1347−1358.
59. Shai, Y. (2002) Mode of action of membrane active antimicrobial peptides, *Biopolymers 66*, 236−248.
60. Matsuzaki, K., Murase, O., Tokuda, H., Funakoshi, S., Fujii, N., and Miyajima, K. (1994) Orientational and aggregational states of magainin 2 in phospholipid bilayers, *Biochemistry 33*, 3342−3349.
61. Shai, Y. (1999) Mechanism of the binding, insertion, and destabilization of phospholipid bilayer membranes by a-helical antimicrobial and cell non-selective lytic peptides, *Biochim. Biophys. Acta 1462*, 55−70.
62. Bechinger, B. (2001) Solid-state NMR investigations of interaction contributions that determine the alignment of helical polypeptides in biological membranes, *FEBS Lett. 504*, 161−165.
63. Axelsen, P. H., Kaufman, B. K., McElhaney, R. N., and Lewis, R. N. (1995) The infrared dichroism of transmembrane helical polypeptides, *Biophys. J. 69*, 2770−2781.
64. Lewis, R. N., Zhang, Y. P., Liu, F., and McElhaney, R. N. (2002) Mechanisms of the interaction of alpha-helical transmembrane peptides with phospholipid bilayers, *Bioelectrochemistry 56*, 135−140.
65. Harzer, U., and Bechinger, B. (2000) The alignment of lysine-anchored membrane peptides under conditions of hydrophobic mismatch: A CD, ^{15}N and ^{31}P solid-state NMR spectroscopy investigation, *Biochemistry 39*, 13106−13114.
66. Ueda, H., Kimura, S., and Imanishi, Y. (1998) Incorporation of hydrophobic helix-bundle peptides into lipid bilayer membranes facilitated by a peptide-umbrella structure, *Chem. Commun. 3*, 363−364.
67. Wimley, W. C., and White, S. H. (2000) Designing transmembrane alpha-helices that insert spontaneously, *Biochemistry 39*, 4432−4442.
68. Bechinger, B. (1996) Towards membrane protein design: pH dependent topology of histidine-containing polypeptides, *J. Mol. Biol. 263*, 768−775.
69. Huang, H. W. (2000) Action of antimicrobial peptides: Two-state model, *Biochemistry 39*, 8347−8352.
70. Bechinger, B., Skladnev, D. A., Ogrel, A., Li, X., Swischewa, N. V., Ovchinnikova, T. V., O'Neil, J. D. J., and Raap, J. (2001) ^{15}N and^{31}P solid-state NMR investigations on the orientation of zervamicin II and alamethicin in phosphatidylcholine membranes, *Biochemistry 40*, 9428−9437.
71. Chen, F. Y., Lee, M. T., and Huang, H. W. (2002) Sigmoidal concentration dependence of antimicrobial peptide activities: a case study on alamethicin, *Biophys. J. 82*, 908−914.
72. Vogel, H. (1987) Comparison of the conformation and orientation of alamethicin and melittin in lipid membranes, *Biochemistry 26*, 4562−4572.
73. Yang, L., Harroun, T. A., Weiss, T. M., Ding, L., and Huang, H. W. (2001) Barrel-stave model or toroidal model? A case study on melittin pores, *Biophys. J. 81*, 1475−1485.
74. Toraya, S., Nishimura, K., and Naito, A. (2004) Dynamic structure of vesicle-bound melittin in a variety of lipid chain length by solid-state NMR, *Biophys. J. 87*, 3323−3335.
75. Stankowski, S., Schwarz, U. D., and Schwarz, G. (1988) Voltage-dependent pore activity of the peptide alamethicin correlated with incorporation in the membrane: salt and cholesterol effects, *Biochim. Biophys. Acta 941*, 11−18.

BI050866N